Relating Eye Activity Measures to Human Controller Remnant Characteristics

Popovici, A; Zaal, Peter; Pool, Daan; Mulder, Max

DOI
10.1016/j.ifacol.2016.10.454

Publication date
2016

Document Version
Accepted author manuscript

Published in
IFAC-PapersOnLine

13th IFAC/IFIP/IFORS/IEA Symposium on Analysis, Design, and Evaluation of Human-Machine Systems
Aug. 30 - Sept. 2, 2016. Kyoto, Japan

Relating Eye Activity Measures to Human Controller Remnant Characteristics

A. Popovici, * **P. M. T. Zaal,** * **D. M. Pool,** ** **M. Mulder** **

* *San Jose State University, NASA Ames Research Center*
(e-mail: {alexandru.popovici, peter.m.t.zaal}@nasa.gov)
** *Delft University of Technology*
(e-mail: {d.m.pool, m.mulder}@tudelft.nl)

Abstract: This study attempts to partially explain the characteristics of the human perceptual remnant, following Levison's representation of the remnant as an equivalent observation noise. Eye activity parameters are recorded using an eye tracker in two compensatory tracking tasks in which the visual information is presented using either a first or second-order visual stimulus. Differences in the two conditions between remnant characteristics, eye activity measures and human operator model parameters are analyzed, using preliminary data from three subjects. Preliminary results show that the second-order visual stimulus introduces changes in both eye activity and remnant model parameters. Although high correlations are observed between remnant gain and blink frequency, between remnant break frequency and eye opening amplitude, and between remnant power and pupil diameter, a definitive conclusion about the perceptual remnant - eye activity characteristics relation cannot be drawn due to the small sample size of the obtained data. This preliminary study is a first step in identifying possible physiological parameters that affect the perceptual human remnant.

Keywords: manual control, human remnant, eye tracking, visual stimulus

1. INTRODUCTION

Linear transfer functions have been widely used to model human manual control behavior and can explain a large part of the mechanism behind it (McRuer and Jex, 1967). The part that can not be modeled by linear transfer functions, also denoted as the remnant, can be attributed to different sources, related to system noise and the exploratory nature of human behavior. A few examples include true observation noise (error in observing the task variables), motor noise, nonlinearities in the human controller (time-varying parameters, time delays), aperiodic sampling of the perceived variables Levison et al. (1969). As Flach (1990) mentions in his work on active psychophysics, the part of control signal linearly correlated to the input gives information on the task and performance of the human operator, whereas the remnant gives insight into the human operator himself. Levison et al. (1969) concluded that the remnant can be represented as an equivalent observation noise injected at the human operator's perceptual level that accounts for most nonlinear behavior. Even though the effects of different variables in the control loop on remnant models have been investigated, there are currently no studies that looked at the effect of changes in physiological eye parameters or in the perception of the displayed variables on the remnant characteristics.

The importance of a better understanding of the human remnant is two-fold. First, identifying and explaining certain sources of the remnant will give a better insight into whether the remnant is of physiological nature, an intrinsic perceptual process, or a combination of both. Second, more complex human operator models that account for human variability and other external environmental factors can be developed in order to better understand and predict human manual control behavior.

The goal of this paper is to investigate the possible relation between changes in physiological eye parameters, and changes in remnant model characteristics. The approach consists of a simple manual tracking task in which an eye tracker is used to capture changes in eye activity parameters. Visual information is presented either as a first or second-order visual stimulus. The remnant is obtained from the error signal measured from the control loop, and modeled as a first-order low-pass filter, according to Levison et al. (1969). The parameters of this filter are then correlated to changes in eye activity parameters. This study provides a preliminary insight on which eye activity measures are more likely to relate to changes in perceptual remnant.

2. BACKGROUND

2.1 Manual Control Task

Figure 1 depicts the control diagram for a typical single-axis manual tracking task. The goal of the human controller is to minimize the error e presented on the display by providing control inputs u which are transformed into the output y through the controlled dynamics H_c. The input forcing function is denoted as f_i. The human con-

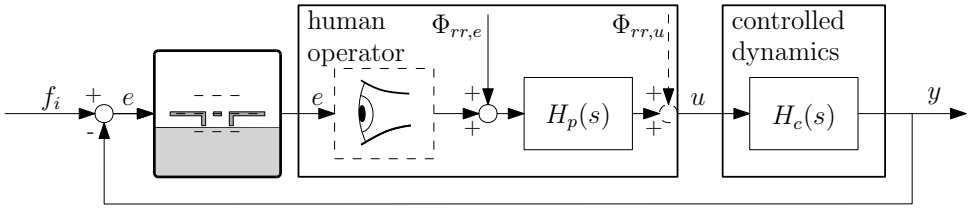

Fig. 1. Control diagram of a manual tracking task.

troller is composed of two parts: a linear transfer function which includes equalization dynamics and neuromuscular limitations, and a remnant signal, $\Phi_{rr,e}$ which accounts for the control behavior not linearly correlated with the frequencies of the forcing function. Note that, since $H_p(s)$ is a linear transfer function, the remnant signal can also be injected in other locations in the control loop, for example at the human operator's control output u, as represented by the signal $\Phi_{rr,u}$ in Figure 1. However, since the goal of this paper is to investigate how changes in perception affect the remnant obtained at the input of the human operator, we chose to add this signal to the perceived error e. This provides a mathematical tool to most directly compare changes in the remnant characteristics with changes in eye activity parameters.

2.2 Remnant modeling

In this study, an investigation on how changes at the perceptual level affect remnant characteristics is carried out. Thus, the need of a model to capture remnant characteristics is evident.

In their early work, McRuer et al. (1965) concluded that the remnant power spectral density is a smooth function of frequency and that its most consistent representation is as an equivalent observation noise injected at the controller's input. Moreover, their work showed that the order of the controlled dynamics has a big impact on remnant characteristics. In addition, Pew et al. (1967) reported that the remnant spectrum is invariant to the bandwidth of the forcing functions and display gain. Later research by Elkind et al. (1971) confirmed these findings, showing that an equivalent observation noise at the human controller's input, normalized by the variance of the error, is invariant to the input characteristics, ultimately meaning that the absolute remnant power scales with the magnitude of the error.

Levison et al. (1969) concluded that, if observation noise signals following Weber's law act on each state of the perceived variables (e, $\dot{e}$), then the equivalent *normalized* remnant spectrum at the perceptual level can be represented by a first-order low-pass filter model. The power spectrum of such a model is given by:

$$|\Phi'_{rr,e}|^2 = \frac{|\Phi_{rr,e}|^2}{\sigma_{\dot{e}}^2} = \frac{K_r}{1 + T_r^2\omega^2}, \qquad (1)$$

where K_r represents the gain of the remnant, T_r is a constant that dictates the ratio in the perception gains on the error rate ($\dot{e}$) and error displacement (e), and ω denotes the frequency vector. Note that the remnant break frequency is given by $\omega_r = 1/T_r$.

This model has been validated by Jex and Magdaleno (1969), in a study that compiled remnant data obtained from numerous experiments. As mentioned before, remnant characteristics are affected by the order of the controlled dynamics. It was experimentally found that, for controlled dynamics of the form $H_c(s) = 1/s(sT_c + 1)$, where the time constant T_c is neither two small nor too large, the remnant model has two identifiable parameters, both K_r and ω_r. However, T_c approaching zero or infinity will also result in the remnant break frequency to become infinity or zero, respectively, meaning that the only identifiable parameter in Equation 1 is the gain K_r. A typical example of a *normalized* remnant spectrum at the human controller's input is shown in Figure 2.

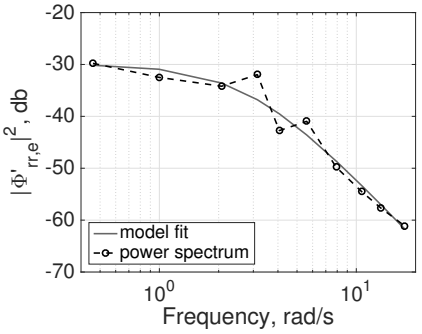

Fig. 2. Power spectrum of the perceptual remnant (K_r = -29.93 db, ω_r = 2.86 rad/s)

3. METHOD

3.1 Changing the Perceptual Remnant

In subsection 2.2, a model for the remnant at the perceptual level of the human operator is introduced. The perceptual channel at the input for the human operator block diagram in Figure 1 is composed of the human's visual system that perceives and processes the task variables (error displacement, error rate) displayed on the screen. Since the interest is to analyze how changes at the perception level affect the behavior of the remnant parameters, some mechanism that induces changes at this level is needed.

In psychophysics, two types of motion stimuli are defined. The visual system extracts motion information from a first-order stimulus using difference in the luminance of objects. However, in case of isoluminance, the visual system relies on differences in contrast, texture or spatial frequency in order to obtain motion information. Multiple studies suggest that motion perception in the two cases relies on different mechanisms inside the visual system (Chubb and Sperling (1989); Ledgeway and Smith (1994)).

Moreover, Jacobs et al. (2010) found correlations between subjective ratings of perceived roughness (given by the texture of an image), pupil diameter, and fixation durations. Pupil diameter increased for higher subjective roughness of the perceived images. Their findings suggest that the perception of different textures can have an impact on certain eye parameters. Since these changes occur at the perceptual level, it then becomes interesting to investigate if different motion stimuli impact the behavior of remnant characteristics and eye activity parameters in compensatory tracking tasks. To this end, the error signal e can be represented using either a first-order or a second-order visual stimulus.

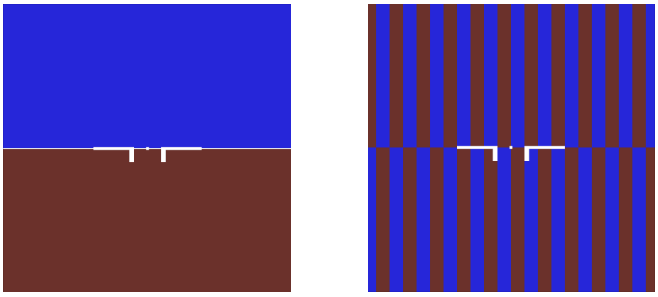

(a) First-order stimulus. (b) Second-order stimulus.

Fig. 3. Representations of error on the display.

Looking at a pitch tracking task, the horizon on the primary flight display in Figure 3(a) is indicated by a white line that has a higher luminance level ($\sim$100 cd/m^2) compared to the background colors ($\sim$20 cd/m^2). In this case, the pitch error movement will be perceived as a first-order stimulus. In Figure 3(b) however, the horizontal white line is absent and the colors of the striped texture are isoluminant. Thus, information about the horizon can only be inferred from the pattern in the texture, at the interface between the two colors. In this case, motion is perceived as a second-order stimulus.

3.2 Experiment

Control Task In the experiment, subjects performed a pitch-tracking task in which the error was presented on a compensatory display, as indicated in the control diagram from Figure 1. In order to analyze both the remnant gain and break frequency, as explained in Section 2.2, the controlled dynamics were set to a single integrator and are given by $H_c(s) = 5/s$. According to the crossover model (McRuer and Jex, 1967), the human operator's linear transfer function then becomes:

$$H_p(s) = K_v e^{-s\tau_v} \frac{\omega_n^2}{\omega_n^2 + 2\zeta_n\omega_n s + s^2}, \qquad (2)$$

where K_v is the visual gain, and τ_v is the time delay in the control loop. The neuromuscular frequency and damping ratio are represented by ω_n and ζ_n, respectively.

The tracking task runs on a system collecting data at 100 Hz. In order to obtain parameter estimates and remnant spectra, a minimum time interval of 81.92 seconds is used. In the remainder of this paper, this time duration will be referred to as a "run". This results in frequency resolution of 0.0767 rad/s. The forcing functions selected had power at frequencies between 0.46 to 17.56 rad/s which cover the range of human control bandwidth (McRuer and Jex, 1967) and allow the identification of the neuromuscular dynamics. Their power spectrum is similar to the forcing functions used in previous manual tracking experiments (Zaal et al. (2015)).

Apparatus The tracking task system is equipped with an LCD screen having a resolution of 1920 x 1200 pixels and refresh rate of 60 Hz. The size of the primary flight display shown on the screen is 15 x 15 centimeters. For eye tracking, a SmartEye Pro© system, collecting data at 60 Hz, is used on a different machine. The tracking task and eye tracker machines communicate via an UDP connection, the eye tracker starting logging data when the tracking task begins. The joystick used in the experiment is a JFx Joystick manufactured by BG Systems, Inc.

Independent Variables To test the differences in perceptual remnant between using first and second-order stimuli in representing the error, the only independent variable in the experiment is given by the two displays shown in Figure 3. The first-order stimulus task will be referred to as the "FO" task and the second-order stimulus task as the "SO" task.

Dependent measures In order to investigate the relation between eye activity, remnant characteristics and human operator's model parameters, several dependent measures are considered. The following variables are obtained from signals in the control loop: the root mean square of the error and control input signals (RMS_e, RMS_u), the human controller model parameters (K_v, τ_v, ζ_n, ω_n), and the remnant characteristics (K_r, ω_r, total power). The physiological measures considered from the eye tracker are blink count, blink duration, eye opening and closing amplitudes and speeds, and pupil diameter.

Participants and Experimental Procedures Three subjects having the average age of 28 years participated in the preliminary experiment. In order to become familiar with the task, each participant performed the tracking task a few times, until the root mean square of their error signal stabilized. Following, the eye tracker was calibrated for each subject in order to make sure that the facial features that allow the recording of the eye gaze and pupilometry are properly recognized. In order to collect the data for the experiment, each subject first performed the FO task for 20 minutes, or 14 runs. After a short break of at least five minutes, the subject performed the SO task for twenty minutes. Participants were instructed to act on each frequency they perceived and to try their best in minimizing the error seen on the display. No material compensation was provided to the subjects for this preliminary study.

3.3 Data Analysis

Human Operator Model Parameters To reduce the bias and increase the accuracy of the parameter estimates, the time series data (e and u) from the 14 runs is averaged. Since the remnant is a stochastic process, the averaging decreases its power, thus increasing the overall signal-to-noise ratio in the control loop. A set of parameters for the

human operator model was obtained for each task, using a time-domain model fitting technique based on maximum likelihood estimation. This method uses a genetic algorithm to determine initial parameter estimates, which are then refined through a gradient-based Gauss-Newton method (Zaal et al. (2009)).

Perceptual Remnant To obtain the power spectrum of the remnant at the perceptual level, a time window of at least one run is needed in order to resolve all frequencies of interest. One remnant spectrum is obtained for each run, then these spectra are averaged in the frequency domain from all 14 runs. This yields one remnant spectrum for each tested condition. The remnant cannot be directly measured during the experiment, since it is a process internal to the human operator. However, it can be retrieved from signals which are directly measured from the control loop, such as e and u (Figure 1). Equations 3, 4 and 5 show how to obtain the remnant spectrum at the location indicated in Figure 1, from the control input u.

$$S_{uu}(\omega_i) = S_{uu,i}(\omega_i) + S_{uu,r}(\omega_i) \tag{3}$$

$$S_{uu,r}(\omega_i) = \sum_{\substack{\omega=\omega_i-2 \\ \omega\neq\omega_i}}^{\omega_i+2} S_{uu}(\omega)/4 = \tag{4}$$

$$= |\Phi_{rr,e}(\omega_i)|^2 \frac{|H_c(\omega_i)|^2}{|1+H_p(\omega_i)H_c(\omega_i)|^2} \tag{5}$$

where S_{uu}, $S_{uu,i}$ and $S_{uu,r}$ represent power spectral densities related to the control input u, $|\Phi_{rr,e}|^2$ the power spectral density of the remnant at the perceptual level, H_p the human controller linear transfer function and H_c the transfer function of the controlled dynamics. Assuming that the power of the remnant is small compared to the one of the input forcing function, H_p can be estimated by $\hat{H}_p(\omega_i) = \frac{U(\omega_i)}{E(\omega_i)}$. At the frequencies of the input forcing function, ω_i, the control signal u has power from the forcing function itself, $S_{uu,i}(\omega_i)$, and the injected remnant, $S_{uu,r}(\omega_i)$, as indicated by Equation 3. Since the remnant is a continuous function of frequency, its power at the location of u at the input frequencies can be obtained as the average power of the control input at the neighboring frequencies, shown in Equation 4. Equation 5 shows how to obtain remnant spectrum at the perceptual level, $|\Phi_{rr,e}(\omega_i)|^2$, from this result. The last step consists in normalizing with the error variance and fitting a model of the form presented in Equation 1 through the power spectrum data in the frequency domain, in order to obtain the remnant gain K_r and break frequency ω_r.

Eye activity parameters As an initial analysis, mean blink count, duration, eyelid opening speeds and amplitudes and pupil diameters were recorded for each task. The mean values from the 14 runs are obtained.

4. HYPOTHESES

We hypothesize that the introduction of a second-order visual stimulus will introduce changes that can be seen in remnant parameters, eye measures and pilot model parameters. Our predictions are:

- The second-order stimulus will make it more difficult to see the higher frequency error motion, resulting in changes in eye measures. The participants are expected to have less frequent blinks due to increased attention. Moreover, the subjective perception of the different texture in the case of the second-order stimulus should have an effect on the pupil diameter.
- More effort in seeing the high frequency error motion with the second-order stimulus will reduce the crossover frequency of the human operator-controlled dynamics system, given by a smaller visual gain. Furthermore, the second-order stimulus is also expected to increase the time delay in the control loop.
- We expect the remnant break frequency to increase in the second-order stimulus task, due to the increased difficulty in discerning the high frequency content of the error.

5. PRELIMINARY RESULTS

The effects of the two types of displays on all the dependent measured are analyzed, in order to verify whether there is a fundamental difference in the dependent measures between the two tasks. Between-subject variability has been removed for all variables.

Performance and Control Activity Figure 4 shows the root mean square of the error and the control input obtained for the two different displays. The different colors represent the three different participants, indicated by red (R), blue (B) and green (G).

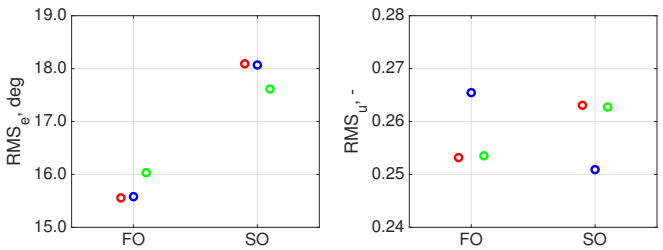

(a) Error signal. (b) Control input signal.

Fig. 4. Root mean square of e and u.

The root mean square of the error increased for all three subjects when controlling the task with the second-order stimulus, as shown in Figure 4(a). Interestingly, participants reported that the second-order stimulus task was much easier to control compared to the first-order stimulus task. This might be related to the fact that the error is less clearly visible in the SO task, especially at higher frequencies of the error, the subjects having the impression that they require less effort in controlling the task. Figure 4(b) shows no consistent differences in the variance of the control input.

Human Operator Model Parameters Figure 5 shows the different pilot model parameters defined in Equation 2. The second-order stimulus task results in a lower visual gain for all subjects, as seen in Figure 5. A lower K_v indicates that the crossover frequency of the open-loop H_pH_c transfer function decreases. Having more difficulty seeing the high frequencies in the error signal might again

be the cause of this behavior, as the subjects control with a lower bandwidth. Although visible for two subjects (R and G), the mean time delay seems to increase by around 40 *ms* for the SO task. The neuromuscular damping increases for the B subject, whereas it decreases slightly for the other two participants, who were probably trying to compensate for the slight increase in the time delay. The neuromuscular frequency has a small decreasing trend for all subjects.

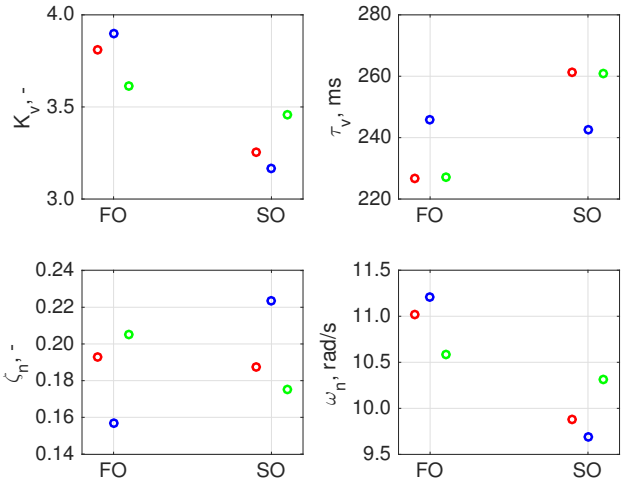

Fig. 5. Human operator model parameters.

Remnant Model Parameters In Figure 6, remnant model parameters, such as the gain and the break frequency, are shown for the two conditions. For two subjects (B and G), the remnant gain K_r is higher for the SO condition, whereas subject R does not show changes, as shown in Figure 6(a). For the remnant break frequency in Figure 6(b), subject R has a higher remnant break frequency for the second-order stimulus. Subject B has a slight increase in remnant break frequency, whereas for G the break frequency decreases. Moreover, Figure 6(c) shows that the total remnant power is higher for all subjects in the SO task. These preliminary results suggest that the increase in remnant power is not due to the same mechanisms in all three subjects.

Eye Activity Parameters Several measured eye parameters that seem to have a correlation to the remnant parameters are shown in Figure 7. The eye closing amplitude seems to have an increasing trend for the task with the second-order visual stimulus for all three participants. The opposite effect is seen in the pupil diameter. Although by a small amount, the pupil diameter seems to decrease for the SO visual stimulus. Even though the luminance of the display in both tasks is identical, the small decrease in the pupil diameter might indicate that the perceived brightness of the display is higher in the SO task (Laeng and Endestad (2012)). For the opening amplitude and blink rates, the parameters do not show the same behavior for all three participants. For instance, only subjects B and G show a slight decrease in blink count, whereas R seems to have a constant blink rate. Furthermore, changes in eye opening amplitude are different for all participants. It is interesting to notice that eye closing amplitude in Figure 7 and the remnant power in Figure 6(c) seem to have similar trends. Similar behaviors can also be seen for the remnant

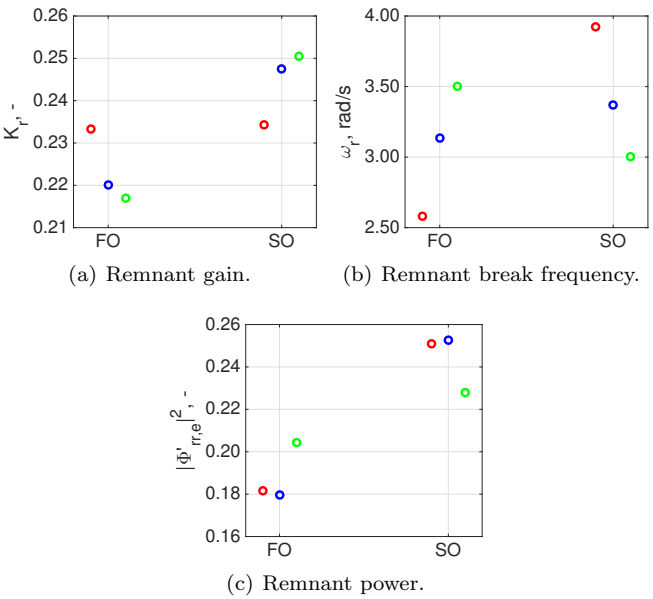

(a) Remnant gain. (b) Remnant break frequency.

(c) Remnant power.

Fig. 6. Remnant model parameters.

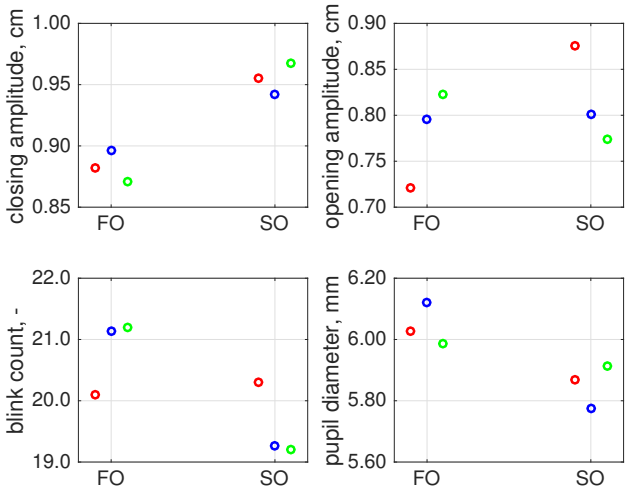

Fig. 7. Eye activity parameters.

gain and blink count. Lastly, the eye opening amplitude seems to correlate with the remnant break frequency.

In order to verify the possible relation between remnant and eye activity parameters, Pearson's correlation coefficients between the variables discussed above are presented in Table 1. Highly significant correlations (to the 0.01 level) are obtained between remnant gain and blink count, remnant break frequency and eye opening amplitude, and remnant power and pupil diameter respectively. Moreover, the remnant gain correlates with the closing amplitude (to the 0.05 level). This is expected since the closing amplitude and pupil diameter present similar but opposite trends.

Table 1. Correlation coefficients between remnant and eye activity characteristics.

	K_r	ω_r	$\lvert\Phi'_{rr,e}\rvert^2$
closing amplitude	0.81*	0.32	0.8
opening amplitude	−0.19	0.99**	0.59
blink count	−0.99**	0.22	−0.59
pupil diameter	−0.71	−0.46	−0.95**

6. DISCUSSION

Performance degraded when using the second order stimulus for all three subjects, whereas no major differences were found in the control input variance. The second-order visual stimulus resulted in a lower visual gain, human operator controlling with lower bandwidth. For two of the subjects, the overall time delay in the control loop increased by $\sim$40 ms in the SO task. These preliminary findings are in agreement with two of the formulated hypotheses.

The remnant gain increased for two of the three subjects in the SO task. It was hypothesized that the break frequency would increase since higher nonlinear behavior was expected due to the introduction of the second-order visual stimulus. However, the remnant break frequency increased for only one subject, remained approximately constant for another and decreased for the last subject. Interestingly, the total remnant power was higher in the SO task for all three subjects, suggesting that the mechanism behind the increased nonlinear behavior in the SO task is different for each participant.

We hypothesized a decrease in blink frequency, together with a change in pupil diameter with the introduction of the second order stimulus. A small decrease in pupil diameter is seen for all subjects; however, it is unclear whether this change is driven by the perceived spatial features of the display, a change in the perceived total brightness or a combination of the two. Blink frequency decreased slightly for two subjects and remained constant for the third. Closing amplitude increased for all subjects, and changes in opening amplitude were different for all subjects.

A preliminary correlation analysis on the limited data available showed high correlations between remnant characteristics and some of the measured eye activity parameters. Remnant gain correlated highly with blink frequency, remnant break frequency with eye opening amplitude, and total remnant power with pupil diameter. It is important to note that the high values of the correlation coefficients might be due to the very small sample size (six data points). Testing more participants is required to verify if these correlations are meaningful.

The second order visual stimulus proved to induce changes in the human operator's model parameters, as indicated by a significant reduction in the visual gain, suggesting that higher frequencies were more difficult to see. Since the remnant is obtained from the signals circulating in the loop, this effect would implicitly change remnant characteristics. It is then difficult to draw conclusions whether the changes in remnant are due to changes in eye parameters or the different nature of the error representation itself. A better option would then be to keep the error representation identical and create changes in the eye parameters in different ways. For example, an experiment could be designed in which the pupil diameter can be reduced by altering the brightness of display.

7. CONCLUSION

A preliminary experiment was performed in order to analyze the relation between changes in physiological parameters and remnant model characteristics. Three participants performed two 20-minute long tracking tasks in which the error was presented as either a first-order or a second-order visual stimulus. An eye tracker was used to measure changes in eye activity parameters. Although remnant characteristics highly correlated with some of the measured eye parameters, no definitive conclusion can be drawn due to the small sample size of the analyzed data. However, the results from this study provide an initial direction for further research looking at the physiological origins of the human perceptual remnant.

REFERENCES

Chubb, C. and Sperling, G. (1989). Two motion perception mechanisms revealed through distance-driven reversal of apparent motion. *Proceedings of the National Academy of Sciences*, 86(8), 2985–2989.

Elkind, J.I., Levison, W.H., and Ward, J.L. (1971). Studies of multivariable manual control systems:a model for task interference.

Flach, J.M. (1990). Control with an eye on perception: precursors to an active psychophysics. *Ecological Psychology*, 2(2), 83–111.

Jacobs, R., Renken, R., Thumfart, S., and Cornelissen, F.W. (2010). Different judgments about visual textures invoke different eye movement patterns. *Journal of Eye Movement Research*, 3(4), 1–13.

Jex, H.R. and Magdaleno, R.E. (1969). Corroborative data on normalization of human operator remnant. *Man-Machine Systems, IEEE Transactions on*, 10(4), 137–140.

Laeng, B. and Endestad, T. (2012). Bright illusions reduce the eye's pupil. *Proceedings of the National Academy of Sciences*, 109(6), 2162–2167.

Ledgeway, T. and Smith, A.T. (1994). Evidence for separate motion-detecting mechanisms for first-and second-order motion in human vision. *Vision research*, 34(20), 2727–2740.

Levison, W.H., Baron, S., and Kleinman, D.L. (1969). A model for human controller remnant. *Man-Machine Systems, IEEE Transactions on*, 10(4), 101–108.

McRuer, D.T., Graham, D., Krendel, E., and Reisener Jr, W. (1965). Human pilot dynamics in compensatory systems: theory, models and experiments with controlled element and forcing function variations. *Wright-Patterson AFB (OH): Air Force Flight Dynamics Laboratory*.

McRuer, D.T. and Jex, H.R. (1967). A review of quasi-linear pilot models. *Human Factors in Electronics, IEEE Transactions on*, (3), 231–249.

Pew, R., Duffendack, J., and Fensch, L. (1967). Sine-wave tracking revisited. *Human Factors in Electronics, IEEE Transactions on*, HFE-8(2), 130–134.

Zaal, P.M.T., Popovici, A., and Zavala, M.A. (2015). Effects of false tilt cues on the training of manual roll control skills. In *AIAA Modeling and Simulation Technologies Conference*, 0655.

Zaal, P.M.T., Pool, D.M., Chu, Q., Mulder, M., Van Paassen, M., and Mulder, J.A. (2009). Modeling human multimodal perception and control using genetic maximum likelihood estimation. *Journal of Guidance, Control, and Dynamics*, 32(4), 1089–1099.